Experimental study and modeling of biomass char gasification kinetics in a novel thermogravimetric flow reactor

Maria Cortazar[a], Gartzen Lopez,[a,b], Jon Alvarez[c], Aitor Arregi[a], Maider Amutio[a], Javier Bilbao[a] and Martin Olazar[a]

[a]Department of Chemical Engineering, University of the Basque Country UPV/EHU, P.O. Box 644 - E48080 Bilbao (Spain). gartzen.lopez@ehu.eus

[b]IKERBASQUE, Basque Foundation for Science, Bilbao, Spain

[c]Department of Chemical and Environmental Engineering, University of the Basque Country UPV/EHU, Nieves Cano 12, Vitoria-Gasteiz, 01006, Spain

Keywords

Biomass; char; CO_2 ; gasification; kinetics; MRPM

Highlights

- A thermogravimetric flow reactor was developed for analyzing gasification kinetics
- The effect of CO_2 concentration and temperature on char gasification was studied
- Five different models were tested for the fitting of experimental results
- The modified random pore model is the one of best fit to the experimental data

Abstract

This work pursues the validation of a new reactor for the evaluation of char gasification kinetics. This novel reactor allows continuous gas flow through the fixed bed sample and accurately monitoring the mass loss throughout the reaction. Accordingly, this

thermogravimetric flow reactor has a great potential for the analysis of different thermochemical processes, such as pyrolysis and gasification of solid feedstocks. In this paper, the gasification of pine sawdust char was carried out and the effect carbon dioxide concentration (10 and 100 vol%) and temperature (800, 850 and 900 ºC) have on char gasification kinetics was assessed. The experimental results were fitted to five different kinetic equations, i.e., homogeneous model (VM), shrinking core model (SCM), *n*th order model, random pore model (RPM) and modified random pore model (MRPM), and the best-fit parameters (frequency factor, activation energy, adjustable parameters and fitting error) were obtained for each model. The modified random pore model provides the best fit to the experimental data. The new thermogravimetric flow reactor allows obtaining rigorous kinetic results, which is clear evidence that the reactor is suitable for studying char gasification kinetics under CO_2 atmosphere.

1. Introduction

In the current energy scenario, an efficient use of clean renewable energy sources is mandatory to tackle the global warming and climate change. Biomass stands out as one of the best alternative energy candidates to produce heat, power and biofuels without contributing to a net rise in CO_2 level [1-4].

Amongst all the thermochemical routes to convert biomass into valuable products, gasification is the most promising one, as it may allow a sustainable production of syngas, which could be used as fuel or intermediate in the production of other fuels and chemicals [5-8]. However, the high tar contents in the syngas restrict its viability for use in industrial processes [9-12]. The main reaction steps involved in biomass gasification are drying, pyrolysis, heterogeneous char gasification and homogeneous reactions undergone by pyrolysis volatiles, i.e., reforming, cracking and Water Gas Shift (WGS)

reactions. Char gasification reactions are very slow even at standard gasification temperatures. This is especially true for CO_2 gasification, which is between 2 and 5 times slower that steam gasification [13, 14]. Thus, char gasification is the controlling step in biomass gasification, i.e., its reaction rate is much slower than the other reactions involved in biomass gasification [6, 15-18]. Therefore, the reactor should be designed in order to attain the gas and solid residence times required for high tar and char conversions, and therefore enhance the overall process efficiency. Accordingly, a deep knowledge of the kinetic rate under the varying conditions in the reactor is crucial for the design and optimization of the gasifier [19, 20].

The heterogeneous char gasification reactions are controlled by the following process parameters: temperature, partial pressure of the gaseous reactant, process pressure and the chemical and physical properties of the char [21]. The mechanism of char-CO_2 reactions have been extensively studied by experimental techniques [22, 23] or computational chemistry [24, 25]. The char-CO_2 reaction is often used to test the reactivities of different types of chars produced in different processes and from different parent coals or biomasses [26]. Char reactivity is modeled by adsorption/desorption reaction mechanisms based on the turnover concept, wherein the carbon atoms that desorb from the carbonaceous matrix (creating gas-phase species) expose underlying carbon atoms that become free carbon sites, which are available for adsorption of gas-phase species [27]. Char-CO_2 mechanisms depend on the chemical composition of the original biomass, conditions used to produce the char, structure of the char (particle size, porosity, surface area and pore size distribution) and catalytic effect of the ashes and their site dispersion degree. All these factors influence the accessibility of CO_2 to the carbon active sites. In fact, the gasification rate is controlled by the available carbon active sites rather than the reactant gas conditions [28, 29].

Char gasification kinetics has been extensively studied by TGA (thermogravimetric analysis), as it allows easily obtaining reliable kinetic results under different operating conditions (pressure, particle size, heating rate, reactive gas concentration, temperature) [30-35]. TGA measurements are usually conducted using small and fine particle char samples, and consequently heat transfer and internal mass transfer resistances are negligible. TGA devices have been widely used to study the kinetics of pyrolysis processes by coupling them to mass spectrometers (MS), as is the case of Py-GC/MS devices. In this set-up, the sample is heated until decomposition to produce smaller molecules, which are separated by gas chromatography and detected using mass spectrometry [36-42]. Macro-TGA devices have also been employed to investigate char gasification reactivity [43-46]. The two techniques provide complementary information about reaction mechanisms involved in char gasification. Unlike conventional TGA devices, macro-TGA devices have the advantage of their larger experimental scale: they handle larger sample amounts and bigger particle sizes. Furthermore, when preparing a sample for a conventional TGA, size-reduction processes may modify the structural and chemical composition, and change the fibrous texture and heterogeneous dispersion of catalytic minerals, which vary depending on the biomass particle size [43, 45]. Moreover, the absence of a gas flow through the sample bed may also cause remarkable external mass transfer limitations on the char particles, especially under high reaction rates. Thus, deviations in the assessment of reaction kinetics may be introduced by using both TGA and macro-TGA devices [47, 48], especially for heterogeneous reactions like char gasification. In order to obtain char gasification results that can be extrapolated to full scale gasifiers (high heating rates and high heat and mass transfer rates), studies in fluidized beds and similar reactors have been performed [49-54]. Nevertheless, in spite of the high relevance of accurately estimating kinetics, char

conversion rates have been monitored using indirect techniques, such as gas product analysis.

A novel thermogravimetric flow reactor has been developed by our research group in order to study the kinetics of any process associated with weight loss or gain. This new reactor gathers the advantages of both conventional TGA and macro-TG devices, i.e., the gasification behavior of chars could be studied under different temperature programmed conditions. In addition, similarly to macro-TGAs, it may treat big particle sizes and large sample masses, with the advantage that it overcomes some of the shortcomings of these devices, as the gasifying agent passes through the char bed, and therefore the gas-solid contact is improved and mass transfer limitations are reduced. Accordingly, this reactor involves a step forward towards the development of reliable kinetic models for the design and simulation of industrial gasifiers. To our knowledge, the relevant literature only mentions a microfluidized bed thermogravimetric reactor by Li et al. for lignite char gasification [55].

The main objective of this study is to validate an original thermogravimetric flow reactor based on the data obtained for char gasification. Thus, gasification kinetics of char derived from pine wood sawdust was carried at high temperatures under CO_2 atmosphere using this new experimental setup, with the aim of obtaining rigorous kinetic data. Moreover, the experimental results have been fitted to different models and their adequacy has been analyzed. The models chosen for the description of char gasification under steam and CO_2 atmospheres are as follows: homogeneous, shrinking core, *n*th order, random pore and modified random pore models.

2. Materials and methods

2.1. Biomass char production and characterization.

Pine wood derived char was produced by flash pyrolysis conducted in a bench scale plant provided with a conical spouted bed reactor. This plant has been successfully employed in the pyrolysis of other biomasses, such as rice husk, orange wastes, plastics, tires and sewage sludge [56-60]. The scheme of the laboratory scale plant is detailed elsewhere [61, 62].

The experimental setup and process conditions were fine tuned based on previous pyrolysis studies. The char was obtained in continuous regime by feeding 1.2 g min^{-1} of pine sawdust (2-4 mm) at 800 ºC under nitrogen atmosphere. The bed was made up of 100 g of sand with a particle size in the 0.8-1.2 mm range, and 9 L min^{-1} of N_2 were used as spouting medium, which corresponds approximately to 1.5 times the minimum spouting velocity. As char production temperature was high, the size of the original biomass particle (2-4 mm range) significantly decreased throughout the process to a size in the 1-2 mm range.

The conical spouted bed reactor allows removing continuously the char from the bed, which avoids its accumulation during the pyrolysis process [17, 63, 64]. Thus, the removal of char from the reactor was carried out through a lateral pipe placed above the bed surface, making the most of density differences of char and sand particles. Finally, the char samples were stored at room temperature for subsequent kinetic study.

Table 1 shows the main features of both the pine sawdust biomass and the produced char. The ultimate and proximate analyses were carried out in a LECO CHNS-932 elemental analyzer and in TGA Q500IR thermogravimetric analyzer, respectively. Surface area and pore volume were determined by N_2 adsorption–desorption in a Micromeritics ASAP 2012 apparatus.

Table 1. Characterization of the biomass and the char.

	Raw biomass	**Char**
Particle size (mm)	2-4	1-2
Ultimate analysis (wt%)		
Carbon	49.33	84.44
Hydrogen	6.06	3.35
Nitrogen	0.04	0.15
Oxygen[a]	44.54	12.06
Proximate analysis (wt%)		
Volatile matter	73.4	7
Fixed carbon	16.7	92.52
Ash	0.5	0.48
Surface area ($m^2\ g^{-1}$)	-	26.95
Pore volume ($cm^3\ g^{-1}$)	-	0.008

[a]Calculated by difference

2.2. Experimental equipment and procedure

The scheme of the novel apparatus is shown in Figure 1. The experiments were conducted in a quartz tube reactor, which is 26 mm in internal diameter and 300 mm long. The reactor is placed within a radiant oven and temperature was controlled by two thermocouples: one placed in the char bed and other one close to the wall of the electric oven. It should be noted that the former thermocouple was used for control purposes. This way, temperature homogeneity was ensured in the whole reactor. Nitrogen and CO_2 were fed during the experiments and their flow rate was measured by two mass flow meters (Brooks SLA5800), which allowed feeding up to 1 L min^{-1}. These mass flow meters, making up by a gas measuring system and a control solenoid valve, were connected to different PID controllers which operated the solenoid control valves in order to control their mass flow rate. Both gases were fed using flexible pipes in order to avoid any perturbation in the recorded mass signal. Moreover, there is a pressure gauge at the gas inlet pipe to measure the pressure drop through the bed. The char bed was located in the middle section of the reactor, and the reactant gases had enough time

to be preheated before contacting the bed. The weighing system is provided with a precision electronic scale (Kern Plus PLS 420-3F) with an accuracy of ∓0.1 mg. The weighing plate was replaced with a smaller one of 50 mm in diameter and a metallic stand placed over it. This metallic stand has two gas inlets to which the gases used in the runs were connected (nitrogen and CO_2). Moreover, the reactor is coupled to the stand, as it has a hole of the same diameter as that of the reactor external diameter. The joint between the stand and the reactor is sealed with a rubber ring to prevent any gas leakage. As the reactor is coupled to the electronic scale, the weight loss of the sample is recorded every second using a PLC controller.

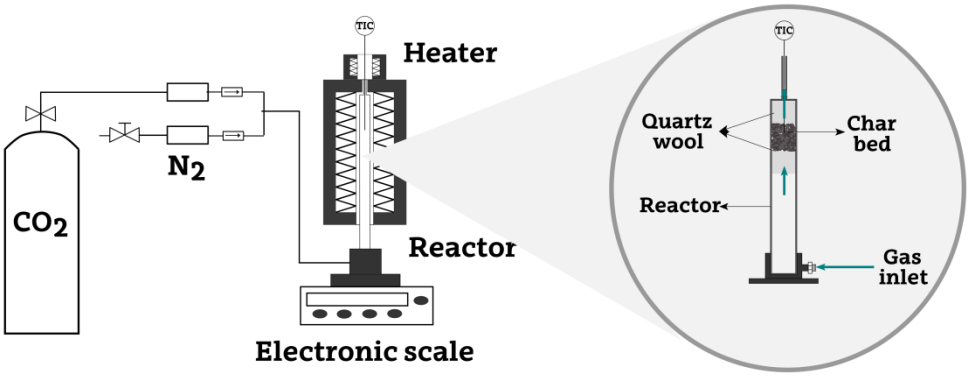

Figure 1. Setup of the thermogravimetric flow reactor with its features in detail.

TGA and macro-TGA devices allow easily obtaining reliable kinetic results under diverse operating conditions. Experiments may be performed under different pressures, particle sizes, heating rates, reactive gas concentrations and temperatures. Unlike conventional TGA devices, the experimental scale of macro-TGA devices is larger and they handle larger sample amounts and bigger particle sizes. Therefore, this novel thermogravimetric flow reactor has the advantages of both TGA and macro-TGA devices in one piece of equipment, i.e., the gasification behavior of chars may be studied under different temperature programmed conditions, it is very simple to use and

many results may be obtained in a reasonably moderate time. Similarly to macro-TGAs, big particle sizes and large mass samples may be treated, with the advantage of overcoming some of the shortcomings of the mentioned devices, i.e., none of the mentioned commercial devices allows the reactant gas crossing the char particles, as the sample is placed into a platinum basket. The absence of gas flow through the sample bed may cause remarkable external mass transfer limitations on the char particles, particularly under high heating rates. Moreover, significant differences between the performance of these devices and industrial equipment in terms of heating rate, reaction environment, gas-solid contact, and so on, may cause deviations in the kinetic results obtained, and therefore their extrapolate to full scale gasifiers is not straightforward. In this thermogravimetric flow reactor, the reactant gases are forced to pass through the char bed. Thus, the gas crosses the bed at high velocity and external mass transfer limitations are therefore minimized. Consequently, the gas-solid contact is optimum. Fluidized beds and similar reactors have been used to obtain char gasification results that are reliable for extrapolating to industrial gasifiers. These reactors allow estimating suitable reaction kinetics, but, in the case of char conversion, indirect techniques (such as gas product analysis) must be used. Directly monitoring the mass loss, as this novel reactor allows, is much easier and more precise than indirect methods to obtain extrapolable data, and this device is therefore especially recommended for these types of processes. Moreover, the novelty of this equipment lies in the way mass loss is recorded. Thus, the base of the reactor is coupled to the metallic stand, and the latter is in turn coupled to the electronic scale. To our knowledge, no similar configuration has been reported in the literature.

At the beginning of each experiment, 1 g of char was place inside the reactor. The reactor has a very fine stainless steel mesh (<90 μm) above the quartz wool to support

the sample, and set the bed at the optimum place in the reactor, as the thermocouple must be located approximately in the middle section of the char bed. Moreover, another piece of quartz wool was also placed above the sample in order to avoid fine dragging during the experiments. Once the reactor was coupled to the metallic stand, and prior to starting each run, the char was loaded, the thermocouple was placed in the char bed and the whole system was tared to start recording weight changes. The total gas flowrate used in all the runs was 500 mL min^{-1}. The effect of CO_2 concentration was assessed for 10 vol% (diluted in nitrogen) and 100 vol%. The sample was initially heated under nitrogen at a heating rate of 10 ºC min^{-1} from room temperature to 800, 850 and 900 ºC and kept at these temperatures for 60 min to ensure they were stable. Then, nitrogen was replaced with CO_2 and temperature was maintained constant until full gasification of the sample. Finally, the reactor was cooled down with nitrogen. Although dynamic runs may have performed, isothermal ones have been conducted, as their result processing is more straightforward.

After the runs, we visually checked there was no sample loss from either the upper or the lower zones and all the ashes were piled on the mesh, i.e., no ashes were retained in the glass wool or reactor inlet. Moreover, the pressure drop values recorded in the experimental set-up were also checked. In all the cases, they were lower than 0.01 atm. Accordingly, the reliability of the kinetic rate parameters obtained is confirmed.

Prior to the set of runs described above, several start-up tests were carried out in this novel reactor to define suitable operating conditions. In these preliminary experiments, different particle sizes, gas flow rates and char masses were tested. The smallest biomass particle size studied was in the 1-1.4 mm range, and the reaction rates were similar to those in this study, even at the highest temperature studied (900 ºC), i.e., when the reaction rate is maximum and is more likely to be diffusional restrictions.

Likewise, experiments with a CO_2 flow rate of 1 L min^{-1} (the maximum allowed by the mass flow meter) were performed, but no significant differences in reaction rate were observed compared those in this study. Therefore, the results obtained in these preliminary tests discard the existence of significant internal or external mass transfer limitations, as the differences observed in char conversions rates with different particle sizes and gas flow rates were negligible.

2.3. Gasification kinetic models

The overall reaction rate of char gasification is described by a general kinetic expression accounting for the evolution of conversion with time as a function of temperature and concentration of the gasifying agent:

$$\frac{dX}{dt} = k(T)P_{CO_2}^{\alpha} f(X) \quad (1)$$

The term *f*(X) in Eq.1 describes the structural and chemical changes during the reaction, which conditions the evolution of char reactivity throughout the gasification process. The conversion, X, is calculated as

$$X = \frac{w_0 - w}{w_0 - w_\infty} \quad (2)$$

where w_0 is the weight of the sample at the beginning of gasification (1 g of char in all the runs), w is the weight of the sample at any time t (recorded throughout the run in the electronic scale), and w_∞ is the weight of the sample at the end of the experiment, corresponding to the weight of the ashes remaining at the end of the gasification process.

Char gasification is a complex heterogeneous reaction in which the conversion rate is highly affected by several parameters, such as pyrolysis step conditions, ash

composition and char porous structure [65]. Up to now, a great number of theoretical and semi-empirical kinetics have been established to describe the evolution of gasification rate with char conversion. These models include some adjustable parameters, whose values are calculated by fitting the experimental results to the models. In this work, five different kinetic models have been applied to describe the change in gasification rate at different temperatures under CO_2 atmosphere. They are as follows: homogeneous model (VM) (Eq.3), shrinking core model (SCM) (Eq.4), *n*th order model (Eq.5), random pore model (RPM) (Eq.6) and modified random pore model (MRPM) (Eq. 8).

The homogeneous model, expressed by Eq.3, is the simplest one. It considers that the reactions take place homogenously in the whole particle (on the surface and inside the particle) and the particle surface area decreases linearly with the conversion [66, 67]. Accordingly, the reaction rate decreases monotonously as the reaction progresses. This model may predict char conversion as a function of time for uncatalyzed char gasification, but acceptable fit is limited to char conversions below 75 %, as the effect of the ashes is much more noticeable at higher conversions [68].

$$\frac{dX}{dt} = kP_{CO_2}^{\alpha}(1 - X) \tag{3}$$

The shrinking core model (Eq. 4) is derived from the homogeneous model. It assumes that char is composed of uniform nonporous grains and the heterogeneous reactions involving char gasification take place on the outer skin of the particles, assuming spherical shape of the grains. This model predicts a decreasing reaction rate, which is proportional to the remaining surface area. The reaction zone moves inwards the char particle centre, leaving behind completely converted material. Thus, at any time, there is an unreacted core of material, which sequentially shrinks [66, 69, 70].

$$\frac{dX}{dt} = kP_{CO_2}^{\alpha}(1-X)^{2/3} \quad (4)$$

The *n*th order model, described by Eq. 5, is an empirical model, i.e., not based on theoretical reaction mechanisms within the char particles. This model may provide a wide variety of conversion vs. time curves depending on the value of reaction order [49, 71, 72].

$$\frac{dX}{dt} = kP_{CO_2}^{\alpha}(1-X)^{n} \quad (5)$$

Compared to the shrinking core model, the random pore model (RPM) correlates the reaction behavior with the internal porous structure, so it could describe complex changes in the surface area of the char particles during the gasification, as shown by Eq. 6. It assumes that the char pores are cylindrical and they have a random size distribution within the particles. This model is able to predict a peak for the reaction rate at conversion levels below 0.4, as it accounts for the competing effects of pore growth and destruction due to coalescence with the adjacent pores, with the latter leading to the progressive collapse of the microporous structure and reduction in the surface area available for reaction [73, 74]. Although it may describe quite well coal and other biomasses char gasification kinetics, several authors found that this model was unsatisfactory for fitting catalytic char gasification [75, 76].

$$\frac{dX}{dt} = k\frac{S_0}{1-\varepsilon_0}P_{CO_2}^{\alpha}(1-X)[1-\psi\, ln(1-X)]^{1/2}$$

$$= k' P_{CO_2}^{\alpha}(1-X)[1-\psi l\, n(1-X)]^{1/2} \quad (6)$$

The parameter ψ in Eqs.6 and 7 is a structural parameter defined as

$$\psi = \frac{4\pi L_0(1-\varepsilon_0)}{S_0^2} \quad (7)$$

where S_0, ε_0 and L_0 stand for the surface area, total volume and length of the porous system made up of randomly coalescing pores. Due to the physical meaning of ψ, this parameter was also fitted.

The modified random pore model (MRPM), given by Eq. 8, is a semi-empirical gasification kinetic model developed by Zhang et al. [77] to overcome the limitations of the original random pore model. This model describes reaction rate profiles with a peak at high conversion values. Therefore, the MRPM could fit the kinetic profile over the entire range of conversion. Thus, the original random pore model was modified for a more general application by introducing a new conversion term with two dimensionless parameters, as given Eq. 8 [20, 75].

$$\frac{dX}{dt} = k' P_{CO_2}^{\alpha}(1-X)[1-\psi l\, n(1-X)]^{1/2}(1+(cX)^{p}) \tag{8}$$

where both *c* and *p* are dimensionless parameters.

2.4. Kinetic model fitting

The fitting of the experimental data to the proposed models was conducted using a program written in MATLAB. The subroutine *fminsearch* provided with the Nelder-Mead simplex algorithm was used to minimize the error objective function (Eq. 9), which allowed determining the parameters of best fit. Moreover, the script calls the subroutine *ode45*, which is based on an explicit Runge-Kutta formula (Dormand-Prince pair) to solve the differential equations and calculate the evolution of conversion with time under different reaction conditions.

$$EOF = \frac{\sum_{j=1}^{L}\left[X_{calculated} - X_{experimental}\right]^2}{L\ \bar{X}^2_{experimental}} \tag{9}$$

where L is the number of the experimental points and X is the average char conversion for the L points considered in the fitting. The results obtained for the different temperatures and CO_2 concentrations were used in the fitting process.

3. Results

3.1. Effect of reaction conditions on gasification rate

In order to validate this novel reactor, the effect temperature and CO_2 concentration have on char gasification rate was assessed. Figure 2a illustrates the char conversion as a function of reaction time in the 800-900 ºC temperature range for a CO_2 concentration of 100 vol%. As temperature was increased from 800 ºC to 900 ºC, the conversion rate increased and the time required to reach full conversion was reduced to approximately to one third. Thus, at 800 ºC the char was fully gasified for 45 min, at 850 ºC for 23 min and at 900 ºC for 15 min. Several authors have reported the sensitivity of carbon conversion to reaction temperature, with high temperatures enhancing char conversion rates [78-81]. However, comparison of literature results for char conversion rate is rather complex, as they are highly dependent on the original biomass composition, the pyrolysis conditions to produce the char and the corresponding gasification conditions [65]. Figure 2b shows the evolution of char conversion for two different CO_2 concentrations of CO_2, 10 vol% and 100 vol% at 900 ºC. As expected, the reduction in CO_2 concentration caused a deceleration in the gasification rate and the time required to reach full conversion is approximately double. As observed in Figure 2, temperature has a more pronounced effect on char conversion than CO_2 concentration. Other authors have reported the same trend for both coal and biomass char gasification. Scala (2005) [82] studied the gasification kinetics of lignite char with CO_2 and reported that the time to reach full conversion was reduced to the tenth part when temperature was increased

from 800 ºC to 900 º, whereas it was only reduced to the forth part when CO_2 concentration was reduced from 20 to 100 vol%.

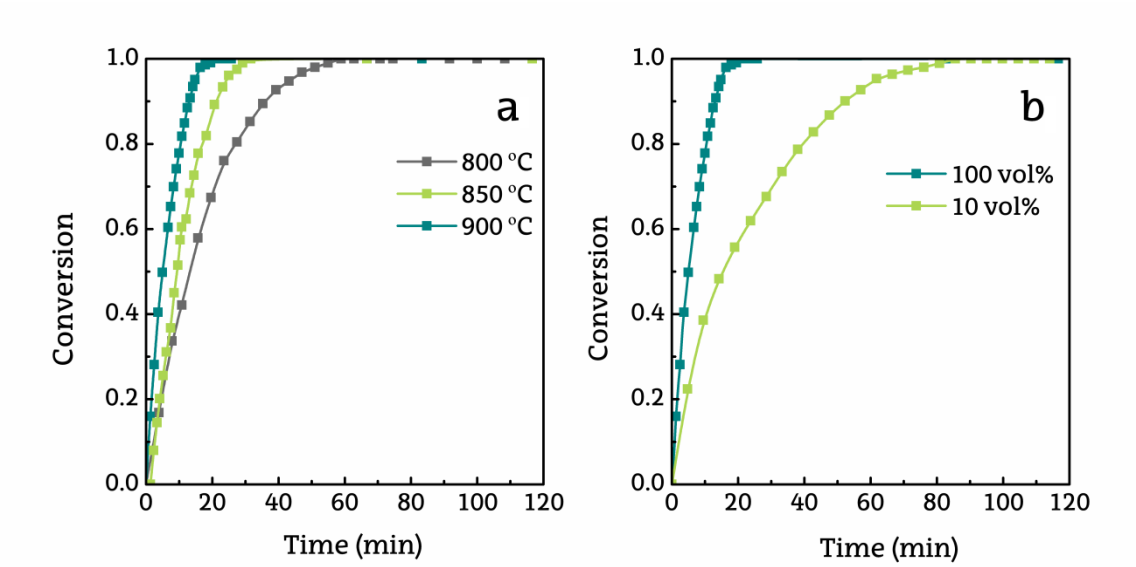

Figure 2. The influence of temperature (CO_2 concentration of 100 % vol.) (a) and CO_2 concentration (at 900 ºC) (b) on char conversion.

3.2. Kinetic analysis

This section deals with the fitting of the experimental data obtained at different temperatures and CO_2 concentrations (following the procedure described in section 2.4) to the homogeneous (Eq. 3), shrinking core (Eq. 4), *n*th order (Eq. 5), random pore (Eq. 6) and modified random pore (Eq. 8) reaction models.

3.2.1. Homogeneous model

Figure 3 shows the fitting of the experimental data to the homogeneous model at the 800-900 ºC temperature range for 100 vol% (a) and 10 vol% (b) of CO_2 concentrations. The best-fit values for the kinetic parameters (values of frequency factor, activation energy, reaction order with respect to CO_2 concentration, other adjustable parameters, and the fitting error) are summarized in Table 2. As shown in Figure 3, the

homogeneous model is not able to accurately predict the biomass char gasification kinetics. Thus, the differences between the experimental and calculated values are evident, which are more remarkable for conversions above 0.8. The fitting obtained for the experiments carried out with 100 vol% of CO_2 is much better than that obtained for 10 vol% of CO_2. Moreover, the fitting of char conversion for the experiments conducted at 800 ºC and 10 vol% of CO_2 is especially poor. Overall, the conversion values calculated for both CO_2 concentrations lead to high deviations, with the error value calculated based on Eq. 9 being of 0.26.

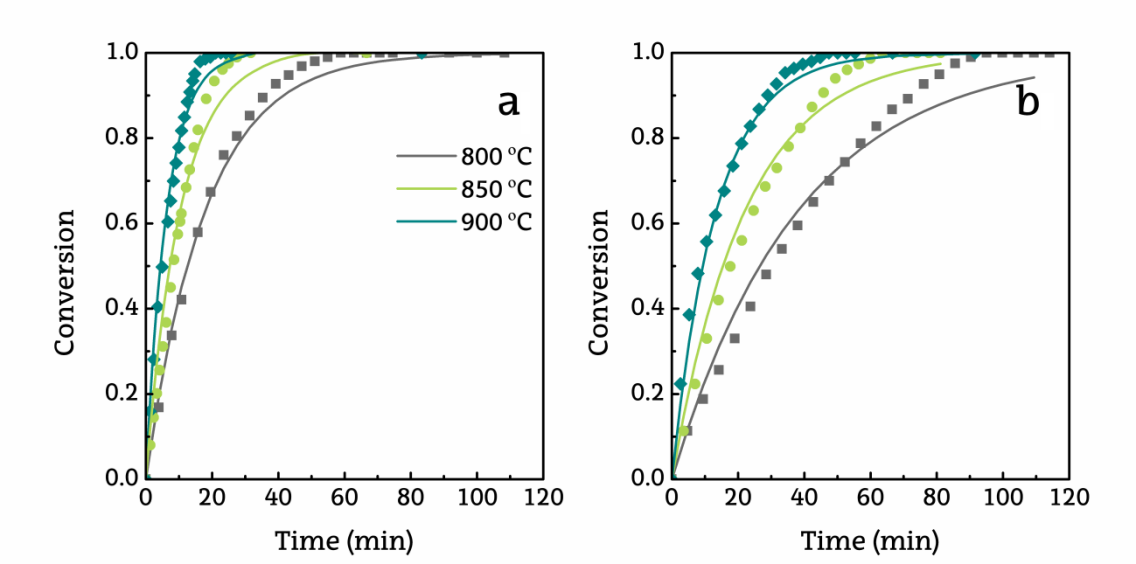

Figure 3. Experimental values and those calculated using the homogeneous model at different temperatures for 100 vol% (a) and 10 vol% (b) of CO_2.

3.2.2. Shrinking core model

The fit of the experimental data to the shrinking core model is shown in Figure 4. As observed, the evolution of the char conversion with time predicted by this model is much closer to the experimental result than the one by the homogeneous model, with the error value being as low as 0.078. However, the values calculated for 800 ºC and 10 vol% of CO_2 still differ considerably from the experimental ones (Figure 4b). The next

step to describe the biomass gasification kinetics lies in considering the reaction order as an adjustable parameter.

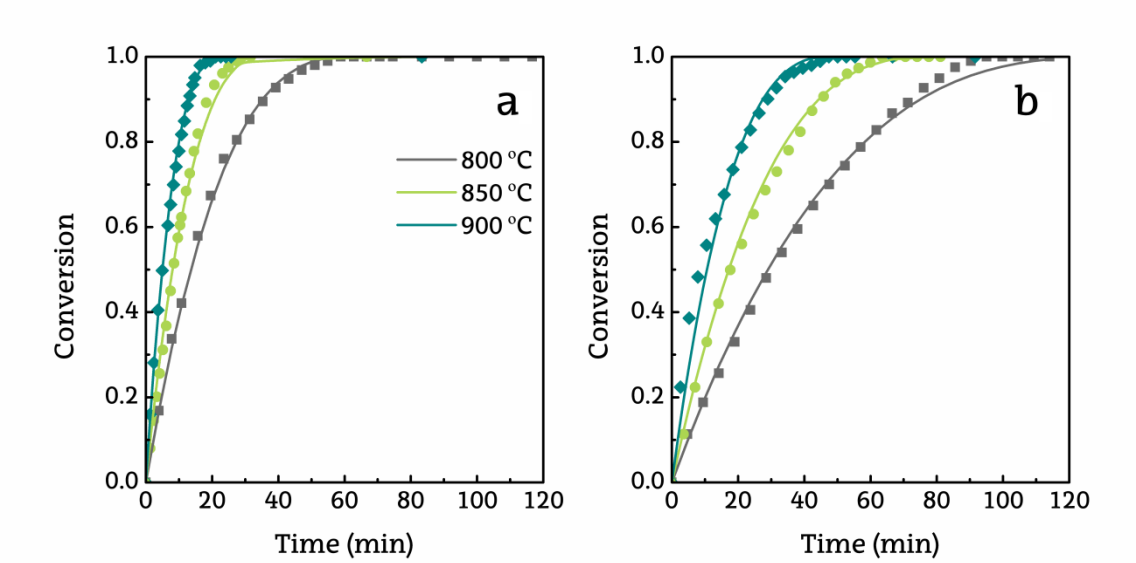

Figure 4. Experimental values and those calculated using the shrinking core model at different temperatures for 100 vol% (a) and 10 vol% (b) of CO_2.

3.2.3. nth order model

Figure 5 compares the experimental data and those calculated using the *n*th order model at different temperatures for 100 vol% and 10 vol% of CO_2. As observed, this model predicts fairly well the experimental results, and provides similar result as those by the shrinking core model (a fitting error of 0.077, Table 2). Regarding the order with respect to char mass, a value of 0.63 is obtained, which is so close to that of the shrinking core model (2/3). Regarding the reaction order with respect CO_2 concentration, the value of best fit is 0.33, which is similar in all the models tested. Different values of the reaction order (with respect to the unconverted char) have been reported in the literature. Thus, Wang et al. (2018) [83] obtained a similar value of *n* (0.58) in the CO_2 gasification of forest residue char and Van de Steene et al. (2011) [46] reported a value of 0.7 in the CO_2 gasification of wood char.

As the *n* value of best fit is slightly lower than that corresponding to the shrinking core model, it is deduced that the evolution of char reactivity (conversion rate divided by the remaining mass of the sample) is slightly more pronounced in the *nth* order model.

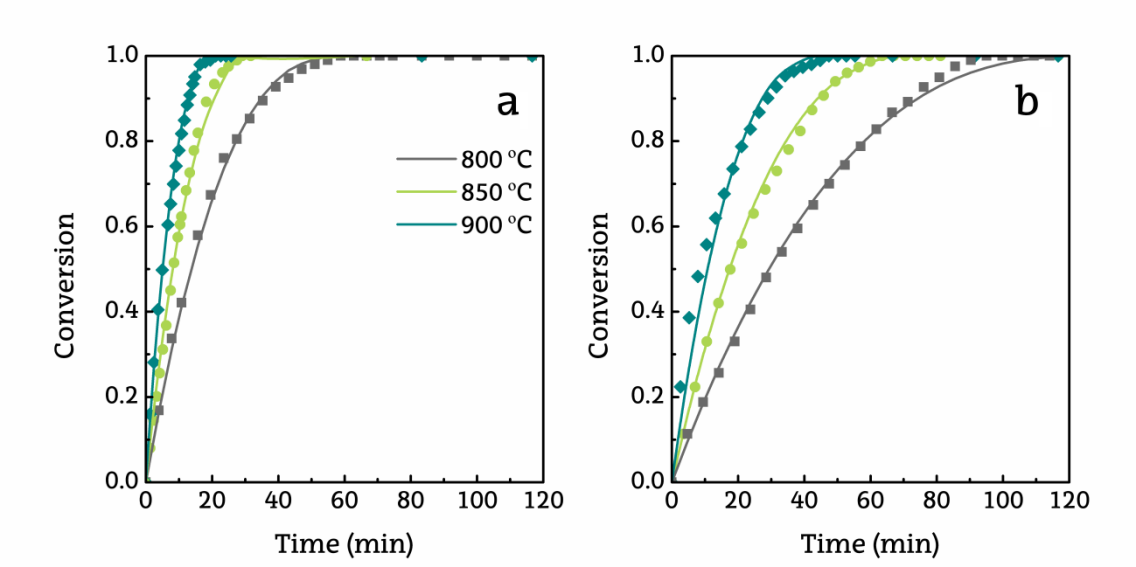

Figure 5. Experimental and calculated results using *n*th order model at different temperatures for 100 vol% (a) and 10 vol% (b) of CO_2.

3.2.4. Random pore model

Figure 6 shows the fitting of the experimental values using the random pore model. As observed in Table 2, the deviation between calculated and experimental results is higher than that corresponding to the shrinking core and *n*th order models (a fitting error of 0.09). However, some authors reported a better description of the reaction kinetics with this model [66, 67, 75, 76, 84, 85].

Although the random pore model may predict the gasification behavior of some chars, such as those derived from coal, it has some limitations to predict the biomass char gasification. Thus, this model fails to suitably describe the reactivity profiles obtained in the gasification of biomass chars catalyzed by the presence of ashes, especially alkali

metals. In fact, the random pore model only foresees reasonable results if the char gasification rate peaks at a conversion level below approximately 0.4 [77, 86]. It seems that pine sawdust char has a reactivity profile influenced by the catalytic effect of the ashes, which cannot be accurately predicted by RPM model.

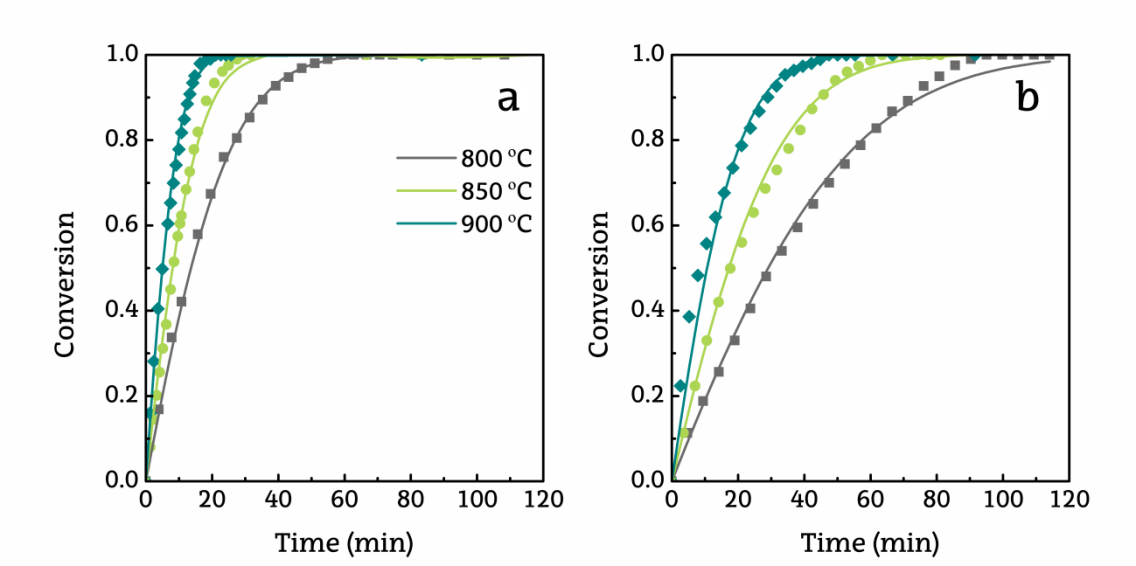

Figure 6. Experimental results and those calculated using the random pore model at different temperatures for 100 vol% (a) and 10 vol% (b) of CO_2.

3.2.5. Modified random pore model

This model was developed in order to overcome the limitation of the random pore model, and was therefore tested with the experimental data obtained in this study for biomass char evolution. It should be note that the parameter Ψ was taken as an adjustable one instead of the fixed value obtained for the random pore model. We believe this value is not representative enough due to the poor fit of the experimental data to the random pore model.

Figure 7 shows the prediction of this model at different temperatures for 100 vol% and 10 vol% of CO_2. As observed, it describes pine sawdust gasification better than the

random pore model (the error lowers from 0.09 to 0.074), which confirms the capability of MRPM to describe reactivity profiles over the entire range of conversion. The error value is slightly lower than those corresponding to the shrinking core and *n*th order models, so it is clearly the best option among the models analyzed.

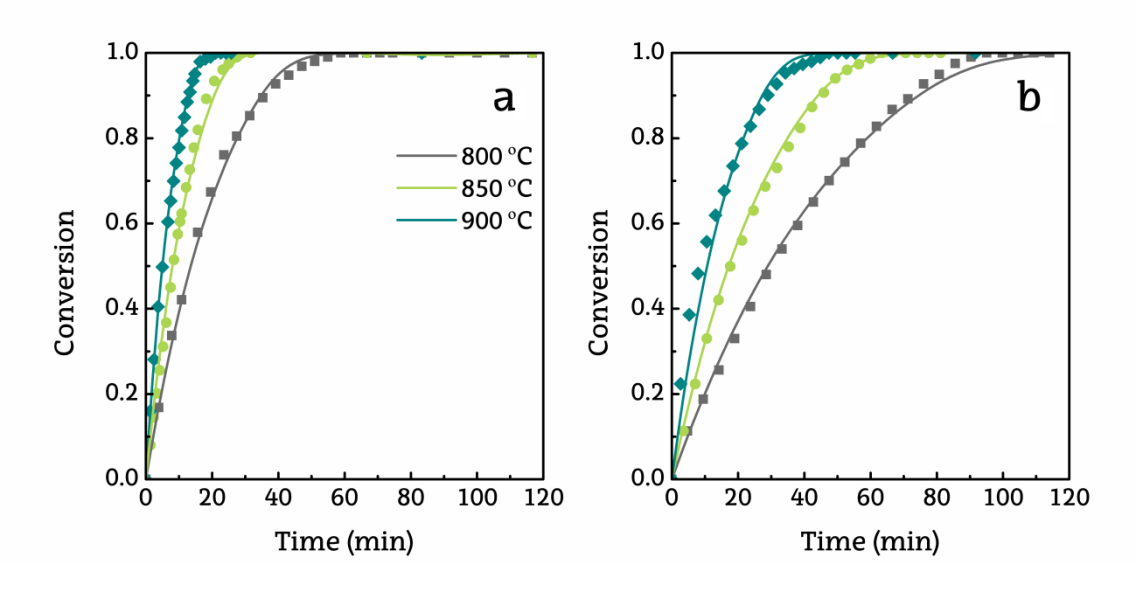

Figure 7. Experimental results and those calculated results using the modified random pore model at different temperatures for 100 vol% (a) and 10 vol% (b) of CO_2.

Concerning the values for the parameters *c* and *p*, they are in the same range as those obtained by Yuan et al. (2011) [87] modeling pine sawdust char gasification with CO_2. They obtained the following dimensionless parameters: c=1.08 and p=3.48.

There are many studies dealing with biomass char gasification kinetics. However, their comparison is not straightforward due to the char characteristics, variety of operating conditions and the different kinetic models tested.

Table 2. Kinetic coefficients, adjustable parameters, fitting errors and coefficients of determination (R^2) for the models tested with a 95% of confidence interval.

Model	ln k_0 (s^{-1})	Ea (kJ mol^{-1})	*n*	*α*	*ψ*	*c*	*p*	*Error*	R^2
VM	5.23∓0.08	108.96∓0.09	-	0.33	-	-	-	0.26	0.981
***n*th**	4.71∓0.06	106.42∓0.08	0.63	0.33	-	-	-	0.077	0.994
SCM	4.81∓0.07	107.11∓0.06	-	0.33	-	-	-	0.078	0.994
RPM	4.7∓0.06	107.49∓0.08	-	0.33	1.68	-	-	0.09	0.993
MRPM	4.82∓0.05	106.8∓0.06	-	0.34	0.33	1.07	5.27	0.074	0.995

It is noteworthy that the activation energy obtained for the five models is similar, around 107 kJ mol^{-1}. A slightly higher value was obtained with the homogeneous model, which should be related to the poor fit of the data to this model. The values of activation energy obtained in this study are rather low compared to those reported in the literature for pine char CO_2 gasification. In fact, the low values of activation energy obtained sugget the kinetic parameters are apparent, which holds true, especially in view of the large char particles used. Thus, the effect of the internal diffusion is much more signficant at high temperatures, and the controlling step may shift from chemical reaction to internal difussion [65]. This fact may reduce the effect of temperature on reaction rate in a given temperature range, and the activation energy obtained is therefore lower than that under kinetic control conditions. However, the experiments performed in this study are under kinetic control conditions, as proven in the series of preliminary runs with smaller particles sizes, in which no significant changes were observed in the measured char conversion rate.

Sircar et al. [84] studied pine wood char gasification with CO_2 in a fixed bed reactor in the 727-897 ºC temperature range and obtained a rather higher activation energy, 125 kJ mol^{-1}. Seo et al. (2010) [67] also obtained similar values for the activation energy, 134 kJ mol^{-1}, in the pine char CO_2 gasification carried out in a fixed bed reactor betwwen 850 and 1050 ºC. Furthermore, much higher values for the activation energy were also reported. Thus, Sadhwani et al. (2016) [75] reported values of 219 kJ mol^{-1} for the CO_2 gasification of pine char carried out in a fixed bed reactor in the 800-975 ºC temperature range.

Regarding Ψ, it is a dimensionless parameter indicating the initial pore structure. In this work, the value of best fit for the parameter Ψ is relatively low, 0.33, which means that the initial porosity of the biomass char is significant, and pore growth during the reaction is negligible, with pore coalescense being the main structural mechanism. Higher Ψ values suggest that the initial porosity of the char is low, and undergoes a significant porous development during the gasification process, as reactions mainly occur on the internal pores of the char [49, 74]. In the literature, the values of Ψ vary in a wide range, even for the same raw biomass, as it depends on char preparation conditions and properties [84]. Kajitani et al. (2002) [88] reported that the value of ψ varied also depending on the gasifying agent. Thus, in the gasification of Australian bituminuous char, they found a value of 3 with CO_2 and H_2O, but 14 with O_2. Fermoso et al. (2009) [89] studied the gasification reactivity of pine char under CO_2 atmosphere in a pressurized theremogravimetric analyser (PTGA), and they reported a value of Ψ slightly higher than obtained in this work, 0.7. Ahmed and Gupta (2011) [90] reported a slightly higher value for Ψ, of around 2.1, in the gasification of woodchip char with CO_2. However, Wang et al. (2016) [91] studied CO_2 gasification kinetics of different

chars and reported much higher values for Ψ, ranging from 5.3 to 187, with the one for the gasification of pine sawdust char being 21.75.

In order to get a better understanding of the different models evaluated in this study, the evolutions of gasification rates foresee with them were compared with the experimental one. Thus, Figure 8 shows the results obtained at 900 ºC with a CO_2 concentration of 100 %. As observed, the MRPM is the only one that suitably predicts the evolution of reaction rate with biomass conversion. It is to note that the experimental results show a clear increase in char reactivity at conversion values above 0.6, with this effect being more acute between 0.8 and full conversion. This kinetic behavior is typical for biomass char, in which the ashes catalyze the gasification reaction at high conversion levels, as their concentration is higher and the inside of the particle is more accessible at these high conversions [26, 65]. The increase in char reactivity at high conversion levels is clearly observed when the experimental reaction rate is compared with that obtained with the homogeneous model (VM), as this model predicts a constant decrease of reaction rate throughout char gasification. Thus, as observed in Figure 8, the experimental reaction rate at high conversion values is markedly higher than that predicted by VM, which is evidence of the increase in char reactivity. RPM is not able to predict the increase in reactivity in the final stage of the gasification. If fact, the MRPM was specifically developed to improve the performance of the conventional RPM in the gasification of biomass chars with significant catalytic effect at high conversion values [77, 92-94]. The SCM and *n*th models predict similar reactivity profiles, but their evolution is not fully satisfactory. It is noteworthy that a good fit in the 0.6-1 range conversion values is critical for a suitable model performance, given that 70 % of the experimental points used in the fitting are in this conversion range. From

this perspective, a significant advantage of the MRPM lies in its potential to predict the whole evolution of reaction rate over the entire conversion range.

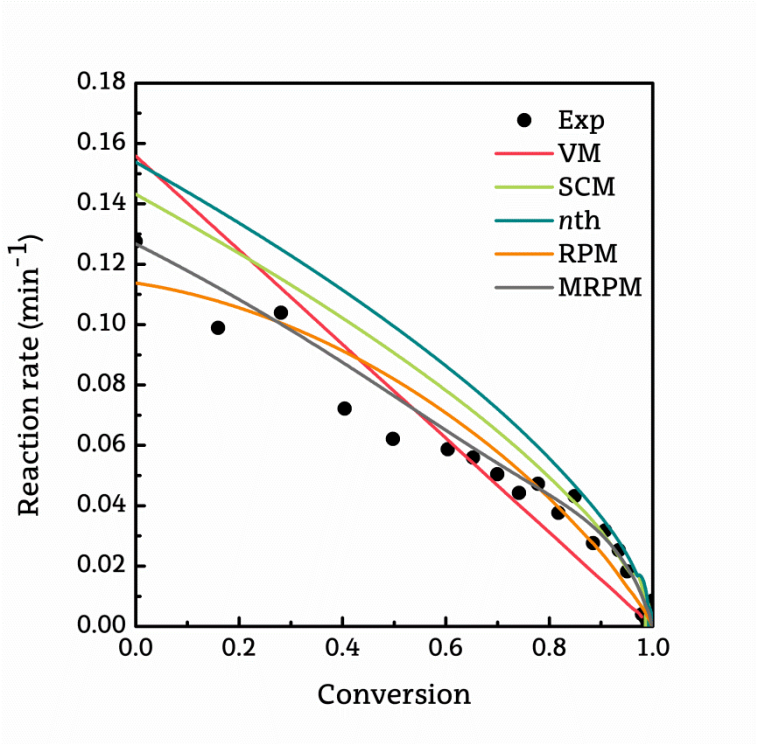

Figure 8. Comparison of experimental reaction rates at 900 ºC with a CO_2 concentration of 100 % and those calculated with the different models under the same conditions.

4. Conclusions

A novel thermogravimentric flow reactor was validated for the evaluation of biomass char gasification kinetics. This reactor combines the capacity for precisely monitoring the mass loss rate throughout the gasification process with a suitable contact between the reactive gaseous stream and the char sample, by minimizing external mass transfer limitations. Thus, this novel reactor allows rigorously determining kinetic data under extrapolable conditions following a much easier and precise procedure than other reactors, thereby being especially useful for these types of processes. Five gas-solid

reaction models were used to analyze their suitability for predicting the kinetics of pine sawdust char gasification with CO_2 obtained in the thermogravimetric flow reactor.

Both temperature and CO_2 concentration have a positive effect on char gasification reaction rate. An increase in temperature from 800 ºC to 900 ºC and CO_2 concentration from 10 to 100 vol.% reduce the time required to reach full conversion to the third part and to the half, respectively.

Among the tested kinetic models, the modified random pore model is the best for predicting the experimental results, with *n*th and shrinking core models providing similar results. The kinetic parameters obtained are as follows: E=107 kJ mol^{-1}, reaction order α=0.34, structural parameter Ψ=0.33 and dimensionless parameters *c*=1.07 and *p*=5.27. The main advantage of this model lies in its capacity for predicting a gasification rate profile with a marked increase in reactivity at high conversion values, which is presumably associated with the catalytic effect of the ashes.

Acknowledgements

This work was carried out with financial support from the Spain's Ministries of Economy and Competitiveness (CTQ2016-75535-R (AEI/FEDER, UE)) and Science, Innovation and Universities (RTI2018-098283-J-I00 (MINECO/FEDER, UE)), the Basque Government (IT1218-19), and the European Union's Horizon 2020 research and innovation programme under the Marie Skłodowska-Curie grant agreement No. 823745. Maria Cortazar also thanks the Basque Government for her research training grant.

References

[1] S.K. Sansaniwal, K. Pal, M.A. Rosen, S.K. Tyagi, Recent advances in the development of biomass gasification technology: A comprehensive review, Renewable Sustainable Energy Rev. 72 (2017) 363-384.

[2] J. Ren, J. Cao, X. Zhao, F. Yang, X. Wei, Recent advances in syngas production from biomass catalytic gasification: A critical review on reactors, catalysts, catalytic mechanisms and mathematical models, Renewable Sustainable Energy Rev. 116 (2019).

[3] H.C. Ong, W. Chen, A. Farooq, Y.Y. Gan, K.T. Lee, V. Ashokkumar, Catalytic thermochemical conversion of biomass for biofuel production: A comprehensive review, Renewable Sustainable Energy Rev. 113 (2019).

[4] C. Zhang, G. Zeng, D. Huang, C. Lai, M. Chen, M. Cheng, W. Tang, L. Tang, H. Dong, B. Huang, X. Tan, R. Wang, Biochar for environmental management: Mitigating greenhouse gas emissions, contaminant treatment, and potential negative impacts, Chem. Eng. J. 373 (2019) 902-922.

[5] Z.A.B.Z. Alauddin, P. Lahijani, M. Mohammadi, A.R. Mohamed, Gasification of lignocellulosic biomass in fluidized beds for renewable energy development: A review, Renewable Sustainable Energy Rev. 14 (2010) X2852-2862.

[6] A. Arregi, M. Amutio, G. Lopez, J. Bilbao, M. Olazar, Evaluation of thermochemical routes for hydrogen production from biomass: A review, Energy Convers. Manage. 165 (2018) 696-719.

[7] Y. Chai, N. Gao, M. Wang, C. Wu, H_2 production from co-pyrolysis/gasification of waste plastics and biomass under novel catalyst Ni-CaO-C, Chem. Eng. J. 382 (2020).

[8] F. Saleem, J. Harris, K. Zhang, A. Harvey, Non-thermal plasma as a promising route for the removal of tar from the product gas of biomass gasification – A critical review, Chem. Eng. J. 382 (2020).

[9] S. Anis, Z.A. Zainal, Tar reduction in biomass producer gas via mechanical, catalytic and thermal methods: A review, Renewable Sustainable Energy Rev. 15 (2011) 2355-2377.

[10] J. Ren, Y. Liu, X. Zhao, J. Cao, Biomass thermochemical conversion: A review on tar elimination from biomass catalytic gasification, J. Energy Inst. (2019).

[11] M.L. Valderrama Rios, A.M. González, E.E.S. Lora, O.A. Almazán del Olmo, Reduction of tar generated during biomass gasification: A review, Biomass Bioenergy 108 (2018) 345-370.

[12] D. Serrano, S. Sánchez-Delgado, A. Horvat, Effect of sepiolite bed material on gas composition and tar mitigation during C. cardunculus L. gasification, Chem. Eng. J. 317 (2017) 1037-1046.

[13] A.R. Mohamed, M. Mohammadi, G.N. Darzi, Preparation of carbon molecular sieve from lignocellulosic biomass: A review, Renewable and Sustainable Energy Rev.14 (2010) 1591-1599.

[14] J.M.V. Nabais, P. Nunes, P.J.M. Carrott, M.M.L. Ribeiro Carrott, A.M. García, M.A. Díaz-Díez, Production of activated carbons from coffee endocarp by CO_2 and steam activation, Fuel Process. Technol. 89 (2008) 262-268.

[15] S. Safarian, R. Unnþórsson, C. Richter, A review of biomass gasification modelling, Renewable Sustainable Energy Rev. 110 (2019) 378-391.

[16] L. Lundberg, P.A. Tchoffor, D. Pallarès, R. Johansson, H. Thunman, K. Davidsson, Influence of surrounding conditions and fuel size on the gasification rate of biomass char in a fluidized bed, Fuel Process. Technol. 144 (2016) 323-333.

[17] J. Alvarez, G. Lopez, M. Amutio, J. Bilbao, M. Olazar, Evolution of biomass char features and their role in the reactivity during steam gasification in a conical spouted bed reactor, Energy Convers. Manage. 181 (2019) 214-222.

[18] X. Gao, Y. Zhang, B. Li, X. Yu, Model development for biomass gasification in an entrained flow gasifier using intrinsic reaction rate submodel, Energy Conversion Manage. 108 (2016) 120-131.

[19] R. Bryan Woodruff, A.W. Weimer, A novel technique for measuring the kinetics of high-temperature gasification of biomass char with steam, Fuel 103 (2013) 749-757.

[20] P. Lahijani, Z.A. Zainal, A.R. Mohamed, M. Mohammadi, Co-gasification of tire and biomass for enhancement of tire-char reactivity in CO_2 gasification process, Bioresour. Technol. 138 (2013) 124-130.

[21] C. Schneider, S. Rincón Prat, T. Kolb, Determination of active sites during gasification of biomass char with CO_2 using temperature-programmed desorption. Part 1: Methodology & desorption spectra, Fuel 267 (2020) 116726.

[22] H. Liu, M. Kaneko, C. Luo, S. Kato, T. Kojima, Effect of pyrolysis time on the gasification reactivity of char with CO_2 at elevated temperatures, Fuel 83 (2004) 1055-1061.

[23] F. Kapteijn, R. Meijer, J.A. Moulijn, Transient kinetic techniques for detailed insight in gas-solid reactions, Energy Fuels 6 (1992) 494-497.

[24] Z.H. Zhu, J. Finnerty, G.Q. Lu, M.A. Wilson, R.T. Yang, Molecular orbital theory calculations of the H_2O-carbon reaction, Energy Fuels 16 (2002) 847-854.

[25] J.F. Espinal, F. Mondragón, T.N. Truong, Thermodynamic evaluation of steam gasification mechanisms of carbonaceous materials, Carbon 47 (2009) 3010-3018.

[26] M.F. Irfan, M.R. Usman, K. Kusakabe, Coal gasification in CO2 atmosphere and its kinetics since 1948: A brief review, Energy 36 (2011) 12-40.

[27] M.B. Tilghman, R.E. Mitchell, Coal and biomass char reactivities in gasification and combustion environments, Combust. Flame 162 (2015) 3220-3235.

[28] K. Jayaraman, I. Gokalp, E. Bonifaci, N. Merlo, Kinetics of steam and CO_2 gasification of high ash coal–char produced under various heating rates, Fuel 154 (2015) 370-379.

[29] K. Jayaraman, I. Gökalp, S. Jeyakumar, Estimation of synergetic effects of CO2 in high ash coal-char steam gasification, Appl. Therm. Eng. 110 (2017) 991-998.

[30] Y. Zhang, P. Geng, Y. Zheng, Exploration and practice to improve the kinetic analysis of char-CO2 gasification via thermogravimetric analysis, Chem. Eng. J. 359 (2019) 298-304.

[31] J. Tanner, S. Bhattacharya, Kinetics of CO2 and steam gasification of Victorian brown coal chars, Chem. Eng. J. 285 (2016) 331-340.

[32] Y. Hu, H. Yu, F. Zhou, D. Chen, A comparison between CO2 gasification of various biomass chars and coal char, Can. J. Chem. Eng. 97 (2019) 1326-1331.

[33] M. Liu, Z. Zhou, Z. Shen, Q. Liang, J. Xu, H. Liu, Comparison of HTSM and TGA Experiments of Gasification Characteristics of Different Coal Chars and Petcoke, Energy Fuels 33 (2019) 3057-3067.

[34] M. Prestipino, A. Galvagno, O. Karlström, A. Brink, Energy conversion of agricultural biomass char: Steam gasification kinetics, Energy 161 (2018) 1055-1063.

[35] K. Umeki, A. Moilanen, A. Gómez-Barea, J. Konttinen, A model of biomass char gasification describing the change in catalytic activity of ash, Chem. Eng. J. 207-208 (2012) 616-624.

[36] T. Menares, J. Herrera, R. Romero, P. Osorio, L.E. Arteaga-Pérez, Waste tires pyrolysis kinetics and reaction mechanisms explained by TGA and Py-GC/MS under kinetically-controlled regime, Waste Manage. 102 (2020) 21-29.

[37] Y. Qiao, B. Wang, P. Zong, Y. Tian, F. Xu, D. Li, F. Li, Y. Tian, Thermal behavior, kinetics and fast pyrolysis characteristics of palm oil: Analytical TG-FTIR and Py-GC/MS study, Energy Convers. Manage. 199 (2019) 111964.

[38] X. Ming, F. Xu, Y. Jiang, P. Zong, B. Wang, J. Li, Y. Qiao, Y. Tian, Thermal degradation of food waste by TG-FTIR and Py-GC/MS: Pyrolysis behaviors, products, kinetic and thermodynamic analysis, J. Cleaner Prod. 244 (2020) 118713.

[39] Y. Zheng, L. Tao, X. Yang, Y. Huang, C. Liu, Z. Zheng, Study of the thermal behavior, kinetics, and product characterization of biomass and low-density polyethylene co-pyrolysis by thermogravimetric analysis and pyrolysis-GC/MS, J. Anal. Appl. Pyrolysis 133 (2018) 185-197.

[40] Z. Ma, J. Xie, N. Gao, C. Quan, Pyrolysis behaviors of oilfield sludge based on Py-GC/MS and DAEM kinetics analysis, J. Energy Inst. 92 (2019) 1053-1063.

[41] C. Quan, A. Li, N. Gao, Research on pyrolysis of PCB waste with TG-FTIR and Py-GC/MS, J. Therm. Anal. Calorim. 110 (2012) 1463-1470.

[42] N. Gao, A. Li, C. Quan, L. Du, Y. Duan, TG–FTIR and Py–GC/MS analysis on pyrolysis and combustion of pine sawdust, J. Anal. Appl. Pyrolysis 100 (2013) 26-32.

[43] A. Fernandez, J. Soria, R. Rodriguez, J. Baeyens, G. Mazza, Macro-TGA steam-assisted gasification of lignocellulosic wastes, J. Environ. Manage. 233 (2019) 626-635.

[44] L.N. Samuelsson, K. Umeki, M.U. Babler, Mass loss rates for wood chips at isothermal pyrolysis conditions: A comparison with low heating rate powder data, Fuel Process. Technol. 158 (2017) 26-34.

[45] C. Guizani, F.J. Escudero Sanz, S. Salvador, The gasification reactivity of high-heating-rate chars in single and mixed atmospheres of H_2O and CO_2, Fuel 108 (2013) 812-823.

[46] L. Van de steene, J.P. Tagutchou, F.J. Escudero Sanz, S. Salvador, Gasification of woodchip particles: Experimental and numerical study of char-H_2O, char-CO_2, and char-O2 reactions, Chem. Eng. Sci. 66 (2011) 4499-4509.

[47] M. Alonso, Y.A. Criado, J.C. Abanades, G. Grasa, Undesired effects in the determination of CO_2 carrying capacities of CaO during TG testing, Fuel 127 (2014) 52-61.

[48] F. Wang, X. Zeng, S. Geng, J. Yue, S. Tang, Y. Cui, J. Yu, G. Xu, Distinctive Hydrodynamics of a Micro Fluidized Bed and Its Application to Gasâ€“Solid Reaction Analysis, Energy Fuels 32 (2018) 4096-4106.

[49] G. Lopez, J. Alvarez, M. Amutio, A. Arregi, J. Bilbao, M. Olazar, Assessment of steam gasification kinetics of the char from lignocellulosic biomass in a conical spouted bed reactor, Energy 107 (2016) 493-501.

[50] S. Tong, L. Li, L. Duan, C. Zhao, E.J. Anthony, A kinetic study on lignite char gasification with CO_2 and H_2O in a fluidized bed reactor, Appl. Therm. Eng. 147 (2019) 602-609.

[51] M. Morin, S. Pécate, M. Hémati, Experimental study and modelling of the kinetic of biomass char gasification in a fluidized bed reactor, Chem. Eng. Res. Des. 131 (2018) 488-505.

[52] J. Kramb, J. Konttinen, A. Gómez-Barea, A. Moilanen, K. Umeki, Modeling biomass char gasification kinetics for improving prediction of carbon conversion in a fluidized bed gasifier, Fuel 132 (2014) 107-115.

[53] M. Morin, S. Pécate, M. Hémati, Kinetic study of biomass char combustion in a low temperature fluidized bed reactor, Chem. Eng. J. 331 (2018) 265-277.

[54] V. Krishnamoorthy, N. Krishnamurthy, S.V. Pisupati, Intrinsic gasification kinetics of coal chars generated in a high-pressure, high-temperature flow reactor, Chem. Eng. J. 375 (2019) 122028.

[55] Y. Li, H. Wang, W. Li, Z. Li, N. Cai, CO2 Gasification of a Lignite Char in Microfluidized Bed Thermogravimetric Analysis for Chemical Looping Combustion and Chemical Looping with Oxygen Uncoupling, Energy Fuels 33 (2019) 449-459.

[56] M. Amutio, G. Lopez, J. Alvarez, M. Olazar, J. Bilbao, Fast pyrolysis of eucalyptus waste in a conical spouted bed reactor, Bioresour. Technol. 194 (2015) 225-232.

[57] J. Alvarez, M. Amutio, G. Lopez, L. Santamaria, J. Bilbao, M. Olazar, Improving bio-oil properties through the fast co-pyrolysis of lignocellulosic biomass and waste tyres, Waste Management 85 (2019) 385-395.

[58] A. Arregi, M. Amutio, G. Lopez, M. Artetxe, J. Alvarez, J. Bilbao, M. Olazar, Hydrogen-rich gas production by continuous pyrolysis and in-line catalytic reforming of pine wood waste and HDPE mixtures, Energy Convers. Manage. 136 (2017) 192-201.

[59] J. Alvarez, B. Hooshdaran, M. Cortazar, M. Amutio, G. Lopez, F.B. Freire, M. Haghshenasfard, S.H. Hosseini, M. Olazar, Valorization of citrus wastes by fast pyrolysis in a conical spouted bed reactor, Fuel 224 (2018) 111-120.

[60] I. Barbarias, G. Lopez, M. Artetxe, A. Arregi, J. Bilbao, M. Olazar, Valorisation of different waste plastics by pyrolysis and in-line catalytic steam reforming for hydrogen production, Energy Convers. Manage. 156 (2018) 575-584.

[61] M. Cortazar, G. Lopez, J. Alvarez, M. Amutio, J. Bilbao, M. Olazar, Advantages of confining the fountain in a conical spouted bed reactor for biomass steam gasification, Energy 153 (2018) 455-463.

[62] M. Cortazar, G. Lopez, J. Alvarez, M. Amutio, J. Bilbao, M. Olazar, Behaviour of primary catalysts in the biomass steam gasification in a fountain confined spouted bed, Fuel 253 (2019) 1446-1456.

[63] L. Santamaria, G. Lopez, A. Arregi, M. Amutio, M. Artetxe, J. Bilbao, M. Olazar, Influence of the support on Ni catalysts performance in the in-line steam reforming of biomass fast pyrolysis derived volatiles, Appl. Catal. B 229 (2018) 105-113.

[64] G. Lopez, A. Erkiaga, M. Amutio, J. Bilbao, M. Olazar, Effect of polyethylene co-feeding in the steam gasification of biomass in a conical spouted bed reactor, Fuel 153 (2015) 393-401.

[65] C. Di Blasi, Combustion and gasification rates of lignocellulosic chars, Prog. Energy Combust. Sci. 35 (2009) 121-140.

[66] D. López-González, M. Fernandez-Lopez, J.L. Valverde, L. Sanchez-Silva, Comparison of the steam gasification performance of three species of microalgae by thermogravimetric-mass spectrometric analysis, Fuel 134 (2014) 1-10.

[67] D.K. Seo, S.K. Lee, M.W. Kang, J. Hwang, T.-. Yu, Gasification reactivity of biomass chars with CO_2, Biomass Bioenergy 34 (2010) 1946-1953.

[68] J. Tang, X. Wu, J. Wang, Kinetic study of steam gasification of two mineralogically different lignite chars: An active site/intermediate model, Fuel 141 (2015) 46-55.

[69] S. Tong, L. Li, L. Duan, C. Zhao, E.J. Anthony, A kinetic study on lignite char gasification with CO_2 and H_2O in a fluidized bed reactor, Appl. Therm. Eng. 147 (2019) 602-609.

[70] L. Nowicki, M. Markowski, Gasification of pyrolysis chars from sewage sludge, Fuel 143 (2015) 476-483.

[71] S. Porada, G. Czerski, P. Grzywacz, D. Makowska, T. Dziok, Comparison of the gasification of coals and their chars with CO2 based on the formation kinetics of gaseous products, Thermochim Acta 653 (2017) 97-105.

[72] J. Alvarez, G. Lopez, M. Amutio, J. Bilbao, M. Olazar, Kinetic Study of Carbon Dioxide Gasification of Rice Husk Fast Pyrolysis Char, Energy Fuels 29 (2015) 3198-3207.

[73] G. Duman, M.A. Uddin, J. Yanik, The effect of char properties on gasification reactivity, Fuel Process Technol 118 (2014) 75-81.

[74] L. Lin, M. Strand, Investigation of the intrinsic CO_2 gasification kinetics of biomass char at medium to high temperatures, Appl. Energy 109 (2013) 220-228.

[75] N. Sadhwani, S. Adhikari, M.R. Eden, Z. Wang, R. Baker, Southern pines char gasification with CO_2—Kinetics and effect of alkali and alkaline earth metals, Fuel Process Technol 150 (2016) 64-70.

[76] G. Wang, J. Zhang, X. Hou, J. Shao, W. Geng, Study on CO2 gasification properties and kinetics of biomass chars and anthracite char, Bioresour. Technol. 177 (2015) 66-73.

[77] Y. Zhang, M. Ashizawa, S. Kajitani, K. Miura, Proposal of a semi-empirical kinetic model to reconcile with gasification reactivity profiles of biomass chars, Fuel 87 (2008) 475-481.

[78] H. Zhang, J. Li, X. Yang, S. Song, Z. Wang, J. Huang, Y. Zhang, Y. Fang, Influence of coal ash on CO2 gasification reactivity of corn stalk char, Renew. Energy 147 (2020) 2056-2063.

[79] Q. He, Q. Guo, L. Ding, J. Wei, G. Yu, CO2 gasification of char from raw and torrefied biomass: Reactivity, kinetics and mechanism analysis, Bioresource Technology 293 (2019) 122087.

[80] X. Yao, Q. Yu, Z. Han, H. Xie, W. Duan, Q. Qin, Kinetics of CO2 gasification of biomass char in granulated blast furnace slag, Int J Hydrogen Energy 43 (2018) 12002-12012.

[81] T. Mani, N. Mahinpey, P. Murugan, Reaction kinetics and mass transfer studies of biomass char gasification with CO_2, Chem. Eng. Sci. 66 (2011) 36-41.

[82] F. Scala, Fluidized bed gasification of lignite char with CO2 and H2O: A kinetic study, Proc. Combust. Inst. 35 (2015) 2839-2846.

[83] L. Wang, T. Li, G. Várhegyi, Ø Skreiberg, T. Løvås, CO_2 Gasification of Chars Prepared by Fast and Slow Pyrolysis from Wood and Forest Residue: A Kinetic Study, Energy Fuels 32 (2018) 588-597.

[84] I. Sircar, A. Sane, W. Wang, J.P. Gore, Experimental and modeling study of pinewood char gasification with CO_2, Fuel 119 (2014) 38-46.

[85] M.P. González-Vázquez, R. García, M.V. Gil, C. Pevida, F. Rubiera, Unconventional biomass fuels for steam gasification: Kinetic analysis and effect of ash composition on reactivity, Energy 155 (2018) 426-437.

[86] L. Ding, Y. Zhang, Z. Wang, J. Huang, Y. Fang, Interaction and its induced inhibiting or synergistic effects during co-gasification of coal char and biomass char, Bioresour. Technol. 173 (2014) 11-20.

[87] S. Yuan, X. Chen, J.Li, F. Wang, CO_2 gasification kinetics of biomass char derived from high-temperature rapid pyrolysis, Energy Fuels 25 (2011) 2314-2321.

[88] S. Kajitani, S. Hara, H. Matsuda, Gasification rate analysis of coal char with a pressurized drop tube furnace, Fuel 81 (2002) 539-546.

[89] J. Fermoso, C. Stevanov, B. Moghtaderi, B. Arias, C. Pevida, M.G. Plaza, F. Rubiera, J.J. Pis, High-pressure gasification reactivity of biomass chars produced at different temperatures, J. Anal. Appl. Pyrolysis 85 (2009) 287-293.

[90] I.I. Ahmed, A.K. Gupta, Kinetics of woodchips char gasification with steam and carbon dioxide, Appl. Energy 88 (2011) 1613-1619.

[91] G. Wang, J. Zhang, J. Shao, Z. Liu, H. Wang, X. Li, P. Zhang, W. Geng, G. Zhang, Experimental and modeling studies on CO_2 gasification of biomass chars, Energy 114 (2016) 143-154.

[92] Y. Zhang, S. Hara, S. Kajitani, M. Ashizawa, Modeling of catalytic gasification kinetics of coal char and carbon, Fuel 89 (2010) 152-157.

[93] H. Liu, C. Luo, M. Kaneko, S. Kato, T. Kojima, Unification of Gasification Kinetics of Char in CO_2 at Elevated Temperatures with a Modified Random Pore Model, Energy Fuels 17 (2003) 961-970.

[94] J. Kopyscinski, R. Habibi, C.A. Mims, J.M. Hill, K_2CO_3-Catalyzed CO_2 Gasification of Ash-Free Coal: Kinetic Study, Energy Fuels 27 (2013) 4875-4883.